

Viscosity Dependence of Polystyrene Local Dynamics in Dilute Solution

Wei Zhu and M. D. Ediger*

Department of Chemistry, University of Wisconsin—Madison, 1101 University Avenue, Madison, Wisconsin 53706

Received September 24, 1996; Revised Manuscript Received December 23, 1996[®]

ABSTRACT: Variable-temperature ^2H NMR T_1 measurements have been performed on backbone-deuterated atactic polystyrene at two Larmor frequencies in four solvents: toluene, *cis*-decalin, dibutyl phthalate, and dioctyl phthalate. The time integral $\langle o \rangle$ of the C–D vector orientation correlation function is extracted from the T_1 data without assuming a specific model for C–D vector reorientation. The hydrodynamic Kramers' theory in the high-friction limit cannot describe the viscosity and temperature dependence of $\langle o \rangle$. In contrast, $\langle o \rangle$ is found to have a power law dependence on solvent viscosity with an exponent of 0.76 ± 0.05 , whether the viscosity is varied by changing solvent or temperature. The internal energy barrier for polystyrene C–D vector orientation is determined to be 14 ± 3 kJ/mol using the power law viscosity dependence. The inapplicability of Kramers' theory is attributed to the lack of a clear separation between the time scales of polymer and solvent motions. As expected on the basis of this explanation, the viscosity exponents for polystyrene and five other polymers are found to correlate with the molecular weight of the side groups.

I. Introduction

The relationship between polymer properties and structures is a major theme of polymer science. The local segmental motions of polymers play an important role in understanding one important structure–property relationship. Dynamics on the scale of a few monomer units depend strongly on the polymer structure and have long been associated with molecular weight independent properties such as T_g , physical aging, and the temperature dependence of the viscosity.

Since the interactions between polymer chains are minimized in dilute solution, this environment has often been used to isolate the intramolecular factors which control local polymer dynamics. Kramers' theory^{1,2} has been the conventional framework for understanding local polymer dynamics in dilute solution. This theory predicts that these dynamics have a linear dependence on solvent viscosity. Recent work^{3–6} has shown that Kramers' theory is not applicable for at least some polymers. Instead of a linear dependence on solvent viscosity, local polymer relaxation times are found to have an apparent power law dependence. The use of Kramers' theory where it is not applicable can lead to serious errors in the determination of the potential energy barrier between different conformational states.^{3,4} This potential energy barrier has been postulated to be one of the most important parameters determining T_g for bulk polymers.

The power law exponent which describes the dependence of local dynamics upon solvent viscosity has been observed to increase with the mass of the polymer side group. For example, in *cis*-1,4-polybutadiene,³ the correlation time for C–H vector reorientation is proportional to solvent viscosity raised to the power 0.33; the exponent is 0.41 for polyisoprene⁴ (PI) and 0.43 for 1,2-polybutadiene⁵ (1,2-PB). This trend has been rationalized by the observation that high-frequency local motions are opposed by a friction which is smaller than that calculated from the zero-frequency viscosity.⁴ This explanation predicts that the viscosity exponent will

become 1 (i.e., Kramers' theory will be applicable) when the side group becomes sufficiently large that its motion is determined by the zero-frequency viscosity. How large must side groups be for Kramers' theory to be applicable? We address this question by performing experiments on polystyrene (PS). Analysis of literature data over a limited viscosity range indicates that PS has a viscosity exponent close to one and thus Kramers' theory is applicable.⁵ Here we check this conclusion with a systematic study covering a wider range of solution viscosities.

We report here the results of ^2H NMR T_1 measurements on backbone-deuterated atactic polystyrene (PS- d_3) in four solvents at two Larmor frequencies. The experimental data are analyzed in the extreme narrowing regime so that no model for the reorientation of C–D vectors needs to be assumed. Our analysis shows that Kramers' theory cannot describe the local dynamics of PS. Instead of having a linear dependence on solvent viscosity η , the time integral $\langle o \rangle$ of the C–D vector correlation function scales with $\eta^{0.76}$. Using the power law viscosity dependence, we found that the activation energy of PS local motions is 11 ± 1 kJ/mol in toluene and 15 ± 2 kJ/mol in other solvents. Reanalysis of literature data on PS solutions gives approximately the same activation energies. The viscosity exponents for various polymers are found to correlate with the mass of the side group.

Comparison of T_1 data at multiple Larmor frequencies also yields information about the shape of the C–D vector orientation autocorrelation function. These results are discussed elsewhere.⁷

II. Experimental Section

Materials. Backbone-deuterated atactic polystyrene (PS- d_3 , $M_w = 56\,000$; $M_n = 27\,000$) was purchased from Cambridge Isotope Lab. Low molecular weight impurities were eliminated from the polymer by fractional precipitation using methyl ethyl ketone as a good solvent and methanol as a poor solvent. The precipitated polymer was placed under vacuum at 373 K for 2–3 h to remove trace solvent. We expect that the purified polymer has M_w somewhat higher than 56 000. For flexible polymers, it has been established that local dynamics are independent of molecular weight when the

[®] Abstract published in *Advance ACS Abstracts*, February 1, 1997.

Table 1. Solvent Viscosities

<i>T</i> (K)	η (cP)	<i>T</i> (K)	η (cP)
Dibutyl Phthalate			
374	2.13	407	1.29
394	1.57	421	1.09
Diocetyl Phthalate			
376	3.82	407	2.15
392	2.78	420	1.76

polymer molecular weight exceeds roughly 10,000.⁸ Therefore the T_1 data presented here represent those of a high molecular weight polystyrene sample.

Toluene, *cis*-decalin, di-*n*-butyl phthalate (DBP), and bis-(2-ethylhexyl) phthalate (DOP) were purchased from Aldrich (purity $\geq 99\%$) and were used as received. Except as noted below, the viscosities of the solvents are reported in the literature.^{9–11} The kinematic viscosities of DBP and DOP from 370 to 420 K were measured using a Cannon-Fenske capillary flow viscometer. Absolute viscosities were calculated assuming that the temperature dependence of DBP and DOP densities follows that given in ref 11. The results are shown in Table 1. At 380 K, the four solvents cover a viscosity range of more than one decade.

With one exception, the polymer concentration in all solutions was of $10 \pm 1\%$ (w/w). Some measurements were performed on a 3% solution in order to determine the dependence of T_1 on concentration. All samples were degassed prior to being sealed under vacuum.

NMR Measurements. Deuterium T_1 measurements were performed at 76.86 and 15.37 MHz on Bruker AM-500 and AC-100 spectrometers, respectively. A standard inversion–recovery–fid pulse sequence was employed. The recovery of the ^2H magnetization was always exponential. The temperature was stable within ± 1 K. T_1 data at 76.86 and 15.37 MHz are reproducible within $\pm 1\%$ and $\pm 4\%$, respectively.

We attempted NMR measurements from the highest possible temperatures to temperatures well below the T_1 minima. The high-temperature limit for each solvent was set either by the solvent boiling point or the NMR probe (limited to 425 K). The low-temperature limit for the 10% PS/toluene solution was set by phase separation at around 233 K. PS/DOP solution and PS/*cis*-decalin solutions were phase-separated below 233 and 268 K, respectively.

Only one peak was observed in ^2H NMR spectra over the entire temperature range of the experiments in all solvents. Therefore the T_1 data measured reflect the average behavior of the methine and methylene deuterons. ^{13}C T_1 measurements on PS solutions indicate that backbone methylene and methine C–H vectors reorient at the same rate.¹² Thus we expect that the two kinds of backbone C–D vectors have very similar dynamics and that the conclusions in this paper apply to both of them.¹³

Data Analysis. The reorientation of a C–D bond may be characterized by its orientation autocorrelation function. NMR T_1 measurements are sensitive to the second-order correlation function:

$$G(t) = \frac{1}{2} \langle 3(\mathbf{e}_x(t) \cdot \mathbf{e}_x(0))^2 - 1 \rangle \quad (1)$$

Here $\mathbf{e}_x(t)$ is a unit vector in the direction of the C–D bond at time t . The brackets indicate an ensemble average. The shape of the correlation function is determined by the specific mechanism of C–D vector reorientation and will be discussed elsewhere.⁷ The rate of C–D vector reorientation may be characterized by a model-independent quantity $\langle \sigma \rangle$,¹⁴ which is the time integral of the correlation function $G(t)$:

$$\langle \sigma \rangle = \int_0^\infty G(t) dt \quad (2)$$

We discuss the dependence of $\langle \sigma \rangle$ on solvent viscosity and temperature in this paper.

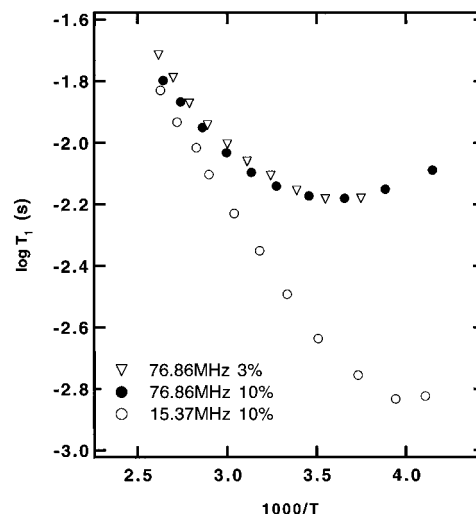


Figure 1. ^2H T_1 values for PS- d_3 in toluene vs temperature. Different symbols represent different concentrations and Larmor frequencies. The 15.37 MHz data above 3 ms ($\log T_1 = -2.52$) are taken to be in the extreme narrowing region.

Deuterium nuclear magnetization is relaxed by electric quadrupole coupling. In the extreme narrowing region, T_1 is related to $\langle \sigma \rangle$ by the following equation:^{15,16}

$$\frac{1}{T_1} = \frac{3}{2} \pi^2 (e^2 q Q / h)^2 \langle \sigma \rangle \quad (3)$$

where $e^2 q Q / h$ is the ^2H quadrupole coupling constant. Consistent with previous work, we chose $e^2 q Q / h$ to be 172 kHz for PS backbone deuterons.^{8,17,18} The uncertainty in this number is expected to be less than 5%. We define the extreme narrowing region by the observation that T_1 is independent of Larmor frequency. Another criterion often used is that $T_1 = T_2$.^{8,19} Because T_2 is sensitive to very low frequency motions such as the reorientation of the whole polymer chain, T_1 is generally not equal to T_2 for polymers. These very slow motions have little effect on T_1 and account at most for the last few percent of the decay of $G(t)$. The $\langle \sigma \rangle$ obtained from eq 3 under these conditions represents an average of all fast motions; i.e., the upper limit of integration in eq 2 is replaced by $(1/\omega_D)$, where $\omega_D/2\pi$ is the deuterium Larmor frequency.

The calculation of $\langle \sigma \rangle$ using eq 3 is not based on any assumption about the shape of the correlation function. For comparison, we have also calculated $\langle \sigma \rangle$ by the integration of modified $\log \chi^2$ correlation functions generated from fitting all the experimental data (including data not in the extreme narrowing region);⁷ these results will be discussed below. $\langle \sigma \rangle$ values used throughout this paper are calculated from eq 3 unless otherwise specified. The conclusions in this paper about $\langle \sigma \rangle$ are believed to be independent of whatever model might be used to fit $G(t)$.

III. Results and Discussion

Figure 1 shows ^2H T_1 values for PS- d_3 in toluene as a function of temperature. We first address the issue of polymer concentration. At 76.86 MHz, to the left side of the T_1 minima, the 3% polymer solution has T_1 values slightly longer than the 10% solution. This indicates that C–D vectors reorient slightly faster in 3% solution than in 10% solution. It has been established that T_1 values for flexible polymers are almost independent of concentration up to 15%,⁸ despite the enormous increase in the solution viscosity. For PS, a threefold concentration increase shortens T_1 by 10% or less. The following discussion is all based on 10% solutions. We expect that the conclusions drawn from this work on 10% solutions will also be applicable to lower concentration solutions.

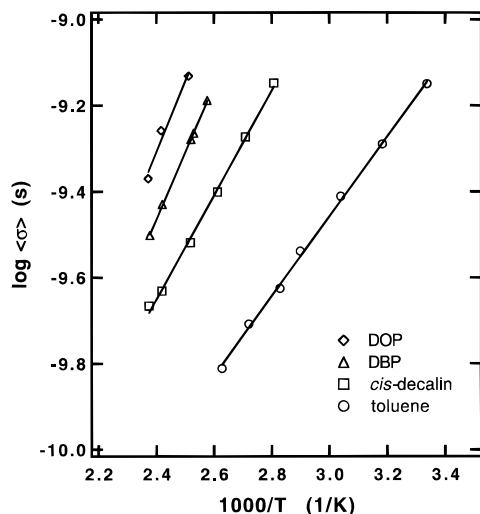


Figure 2. Time integral of C–D vector correlation function $\langle\sigma\rangle$ vs temperature in different solvents. $\langle\sigma\rangle$ is calculated from 15.37 MHz data in the extreme narrowing region (see eq 3).

Figure 1 also allows us to estimate the limits for the extreme narrowing region. At 382 K ($1000/T = 2.62$), T_1 data at two Larmor frequencies are within $\pm 5\%$ of 15 ms, which means that the extreme narrowing condition is approximately met when T_1 is longer than 15 ms at 76.86 MHz. Given that the two Larmor frequencies are different by a factor of 5, we may extend this 15 ms limit by a factor of 5, and approximate the extreme narrowing condition at 15.37 MHz as the region where T_1 is longer than 3 ms. The same criterion has been applied to T_1 data in other solvents; $\langle\sigma\rangle$ values have been calculated from T_1 values at 15.37 MHz using eq 3.

Figure 2 shows the calculated $\langle\sigma\rangle$ versus temperature in different solvents. At a given temperature, higher viscosity solvents such as DBP and DOP naturally show larger $\langle\sigma\rangle$, indicating slower motions. The rest of this paper discusses the data illustrated in Figure 2. All T_1 data may be found in the supporting information.

Inapplicability of Kramers' Theory. Kramers' theory describes the rate at which a particle passes over an energy barrier under the influence of Gaussian random forces.¹ It has often been applied to polymer local dynamics in dilute solution. In this context, and in the high-friction limit, Kramers' theory predicts that^{20–23}

$$\langle\sigma\rangle = A\eta \exp\left(\frac{E_a}{RT}\right) \quad (4)$$

Here A is a constant and E_a is usually interpreted as the average potential energy barrier between conformational states.

Equation 4 can be tested in two ways using data shown in Figure 2. Constant-temperature plots of $\log\langle\sigma\rangle$ vs $\log\eta$ are presented in Figure 3. Since there is no one temperature where $\langle\sigma\rangle$ values are available for all four solvents, we chose two temperatures in order to use data from all solvents, with the data for three solvents being used at each temperature. The slopes of the two lines in Figure 3 are 0.76. This is not consistent with Kramers' theory, which predicts a slope of 1. Thus eq 4 is incapable of describing the viscosity dependence of $\langle\sigma\rangle$ at constant temperature.

Equation 4 may be further tested by varying the temperature. We plot $\log(\langle\sigma\rangle/\eta)$ vs the inverse of temperature in Figure 4. Instead of a master curve of

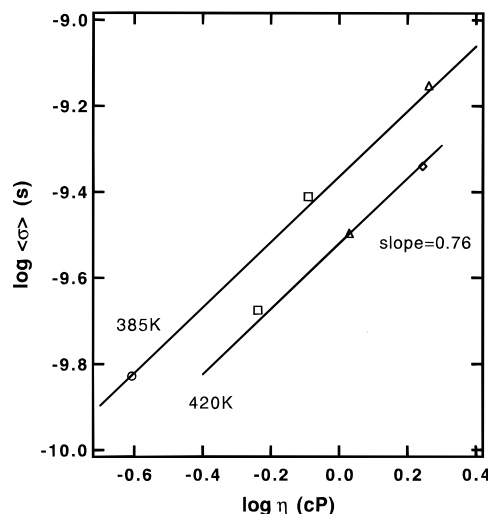


Figure 3. Logarithm of $\langle\sigma\rangle$ vs the logarithm of solvent viscosity at constant temperature. The two lines have a slope of 0.76. In contrast, Kramers' theory in the high-friction limit predicts a slope of 1. Solvent symbols are the same as in Figure 2.

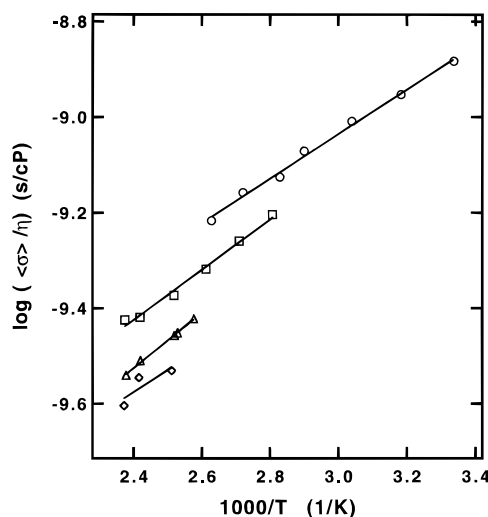


Figure 4. Test of Kramers' theory (eq 4) using C–D vector reorientation times $\langle\sigma\rangle$ in various solvents. Solvent symbols are the same as in Figure 2. Different solvents have different lines, which suggests that Kramers' theory cannot describe the behavior of C–D vector reorientation of PS- d_3 in dilute solution.

all four solvents, as predicted by eq 4, data from the four solvents fall on four different lines. Although one may argue that the preexponential factor A may be different in different solvents, we know of no reason why A should vary with solvent viscosity systematically.

Nonlinear Viscosity Dependence. Previous investigations have found^{3–6} that $\langle\sigma\rangle$ often has a power law dependence on solvent viscosity:

$$\langle\sigma\rangle = A\eta^\alpha \exp\left(\frac{E_a}{RT}\right) \quad (5)$$

Figure 3 has shown that at 420 and 385 K, α is 0.76 ± 0.05 . We may further test eq 5 by varying temperature. Thus we plot $\log(\langle\sigma\rangle/\eta^{0.76})$ vs the inverse of temperature in Figure 5. Data from the four solvents form a master curve. Although not perfect, the power law viscosity dependence does provide a reasonable fit to the experimental data. The average E_a calculated using eq 5 is 14 ± 3 kJ/mol.

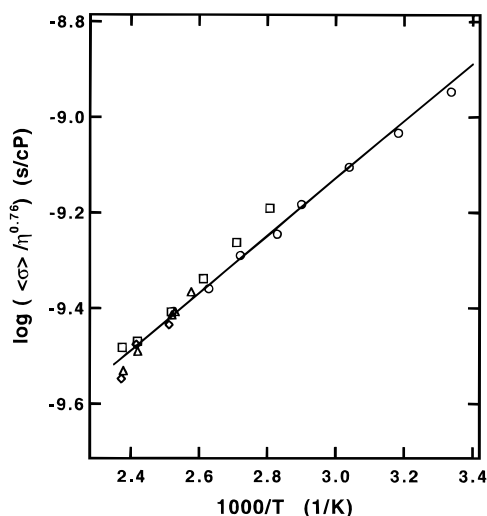


Figure 5. Test of the power law viscosity dependence using the viscosity exponent extracted from Figure 3. Solvent symbols are the same as in Figure 2. Different solvents fall on the same line, indicating that the power law viscosity dependence is a reasonable description of PS local dynamics in dilute solution.

Careful examination of Figure 5 reveals that the local dynamics of PS seem to have slightly different activation energies in different solvents. E_a is equal to 11 ± 1 kJ/mol in toluene, 13 ± 1 kJ/mol in *cis*-decalin, 16 ± 1 kJ/mol in DBP, and 14 ± 3 kJ/mol in DOP. E_a values for PS in DBP and toluene are clearly different. In contrast, E_a does not depend upon solvent for other polymers such as *cis*-1,4-polybutadiene³ and polyisoprene.⁴ The variations observed for E_a values for PS may be due to specific interactions between the polymer and the solvents.

The inapplicability of Kramers' theory is most likely due to the lack of a separation in time scales for the polymer and solvent motions. Kramers' theory is derived from the Langevin equation. One important assumption when applying the Langevin equation is that the system dynamics are significantly slower than the bath dynamics. For the case of a dilute polymer solution, the polymer is the system and the solvent is the bath. If a conformational transition proceeds slowly (relative to the solvent motions), then at each point along the reaction coordinate the solvent is able to equilibrate to the new positions of the chain atoms. In this case the friction impeding the polymer's conformational transition is proportional to the zero-frequency solvent viscosity and the high-friction Kramers' theory should be applicable. For *cis*-1,4 polybutadiene³ and polyisoprene⁴ in dilute solution, it has been shown that local polymer motions are comparable and sometimes even faster than the solvent motions. For PS-*d*₃, it is likely that the time scale separation between polymer and solvent motions is also not large enough to make the Langevin equation valid. We note that for poly(1-naphthylmethyl acrylate) (PNMA),²⁴ whose motions are even slower than PS-*d*₃ in a given solvent, the viscosity exponent α equals 1; i.e., Kramers' theory seems to be applicable for solutions of PNMA.

The above argument is further justified by work on small-molecule isomerization reactions. A functional form similar to eq 5 has been obtained theoretically for such reactions if the solvent is treated as viscoelastic. Grote and Hynes²⁵ generalized Kramers' theory by including the frequency dependence of the friction. Physically this means that the part of the viscosity

which arises from low-frequency motions does not impede motion across the barrier; thus the effective solvent friction in the barrier region is much smaller. Bagchi and Oxtoby²⁶ applied Grote and Hynes' theory to the rate of photochemical isomerization in solution. A power law dependence on solvent viscosity was found, with the solvent exponent ranging from 0.1 to 1. Recent work has extended this approach.²⁷

Another possible reason for the failure of eq 4 may lie in the traditional assumption that the rate of conformational transitions is inversely proportional to the characteristic time $\langle\sigma\rangle$. Recent computer simulations by Moe and Ediger²⁸ have raised doubts about this assumption. Although further investigation is required, our current speculation is that the changes in the relationship between transition rates and $\langle\sigma\rangle$ do not account for the nonlinear viscosity dependence.

In the analysis above, we have only used data from the extreme narrowing regime and have not assumed any model for C–D vector reorientation. It is possible to check our conclusions by fitting all the NMR data (both in and out of the extreme narrowing regime) with a specific model. For this purpose we used the modified $\log \chi^2$ model and calculated $\langle\sigma\rangle$ by integrating the C–D vector correlation function extracted from the fitting. Details may be found elsewhere.⁷ Using $\langle\sigma\rangle$ values extracted from these fits, plots of $\log \langle\sigma\rangle$ vs $\log \eta$ give α values of 0.78 at 420 K and 0.86 at 385 K. The activation energy E_a obtained from the fitting is 16 ± 4 kJ/mol, with 12 kJ/mol in toluene, 18 kJ/mol in *cis*-decalin, and 20 kJ/mol in DBP.

The model-dependent approach agrees with the model-independent approach in a broad sense; i.e., eq 4 is not applicable to PS. In the model-independent approach, the extreme narrowing region can only be defined approximately. In the model-dependent approach, a particular model has to be assumed. This model is not necessarily correct and the fitting is not perfect. For the present, we have more confidence in the model-independent approach. T_1 measurements at a lower Larmor frequency should better define the extreme narrowing region and allow the discrepancy between the activation energies obtained from these two different approaches to be resolved.

Comparison of α for Different Polymers. Although the theoretical prediction of α is not possible at this time, it has been argued⁴ previously that α should depend upon three factors: the moment of inertia, the size of the isomerizing unit, and the curvature of the potential energy surface on the top of barrier. Bigger size, a bigger moment of inertia, and a smaller curvature all lead to a bigger α (up to a limit of 1). While the curvature of the potential is difficult to determine from experimental measurements, the size and the moment of inertia of the isomerizing group correlate roughly with the molecular weight of the polymer side group. Thus we expect that α should increase as the side group molecular weight increases. Figure 6 shows that this is the case. Eventually when the polymer has a very large side group such as poly(1-naphthylmethyl acrylate), $\alpha = 1$ and Kramers' theory is applicable. In the absence of detailed experiments on a given polymer, we suggest that Figure 6 might provide a rough estimate of α . The relationship between α and side group mass might be different for quite flexible side groups.

Comparison to Other Work on PS Solutions. Two groups have previously investigated backbone segmental motions of PS in solution using NMR. Gron-

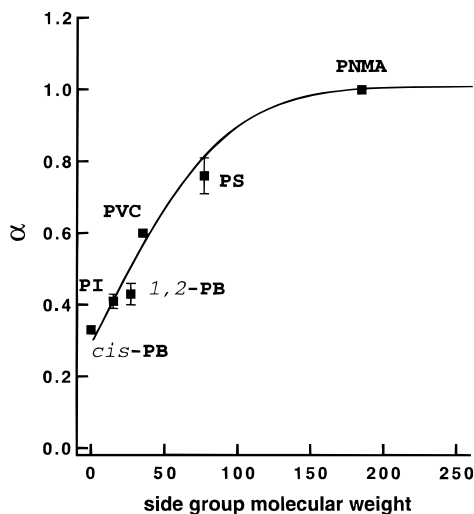


Figure 6. Viscosity exponent α of various polymers vs side group molecular weight. As the molecular weight increases, α increases until it reaches 1. The error bar for *cis*-PB is smaller than the symbol. The α values for PVC and PNMA are model dependent and have undetermined error bars. α is obtained from the following references: *cis*-PB, ref 3; PI, ref 4; 1,2-PB, ref 5; PVC(poly(vinyl chloride)), ref 6; PS, this work; PNMA (poly(1-naphthylmethyl acrylate)), ref 24. The line is drawn to guide the eye.

ski et al.²¹ used ^{13}C NMR T_1 measurements to study 1% PS in toluene and cyclohexane. Such low-concentration solutions could be studied because the PS was 50% ^{13}C enriched at backbone methine carbons. Assuming Kramers' theory, they obtained activation energies of 10.5 kJ/mol in toluene and 15 kJ/mol in cyclohexane. A reanalysis of their data using eq 5 with $\alpha = 0.76$ gives an activation energy of 13 kJ/mol in toluene and 18 kJ/mol in cyclohexane. Grandjean et al.²⁹ performed ^2H T_1 experiments on 16% and 18% PS- d_3 in benzene and in diethyl malonate, respectively. They used Kramers' theory to obtain activation energies of 14 kJ/mol in benzene and 12 kJ/mol in diethyl malonate. Their data cover a limited temperature range and thus the activation energies have reasonably large errors. Reanalysis of these data using the nonlinear viscosity dependence yields an activation energy of 16 kJ/mol in both solvents. All these results are in reasonably agreement with those reported here. In the work reported in refs 21 and 29, specific models were employed to fit the data. It is not known whether other models would give the same results.

The use of Kramers' theory to describe the viscosity dependence of polymer local dynamics can lead to incorrect activation energies. For PS, the viscosity exponent is close to 1; therefore the errors in activation energy generated by assuming Kramers' theory are not large. For polymers with smaller viscosity exponents,^{3–5} Kramers' theory can lead to substantial errors. For PS the dependence of E_a on solvent complicates any attempt to equate this quantity with a barrier in the bulk. For other polymers, E_a is often observed to be solvent independent.

Optical measurements have been performed by Waldow et al. on anthracene labeled PS in six solvents.³⁰ These PS molecules each contained one chromophore covalently bonded into the center of the chain backbone. Time-correlated single-photon counting was employed to monitor the chromophore (anthracene) reorientation in labeled chains. A viscosity exponent α of 0.90 ± 0.05 was found in these experiments. The different α values

found in the optical and the NMR experiments are due to the presence of the chromophore in the optical experiments. Because of this, the length scale of the segmental motions detected in the optical experiments is somewhat larger than that in the NMR experiments (perhaps 5–10 repeat units in the optical experiments and 1–2 repeat units in the NMR experiments). Motion of larger portions of the chain leads to an α closer to unity in the optical experiments. Qualitatively, this is similar to the trend shown in Figure 6. For polyisoprene, the viscosity exponent α was determined to be 0.41 from the NMR measurements⁴ and 0.76 from the optical measurements.³¹

IV. Summary

Deuterium T_1 measurements have been performed on backbone-deuterated PS- d_3 in four solvents. The time integral of the C–D vector orientation correlation function $\langle \sigma \rangle$ has been extracted from T_1 measurements model independently. In contrast to the prediction of Kramers' theory in the high-friction limit, $\langle \sigma \rangle$ is found to be proportional to solvent viscosity η raised to the 0.76 ± 0.05 power, whether the viscosity is varied by changing the temperature or solvent. A very similar result is obtained if the T_1 measurements are analyzed using a model for the description of C–D vector reorientation.⁷ These results fit in well with results from the literature and indicate that the viscosity exponent increases with the mass of the polymer side group.

The internal energy barrier E_a associated with C–D vector orientation was found to be 14 ± 3 kJ/mol. The systematic dependence of E_a upon the solvent identity was not expected and is in contrast to the behavior observed for polyisoprene, *cis*-1,4-polybutadiene, and 1,2-polybutadiene.

Acknowledgment. This research was supported by the National Science Foundation through the Division of Material Research, Polymers Program (Grant DMR-94 24472). We thank Tom Farrar for use of the Bruker AC-100. Some NMR experiments were performed in the Instrument Center of the Department of Chemistry, University of Wisconsin. We thank Marvin Kontney and other staff for assistance.

Supporting Information Available: T_1 data for PS- d_3 in toluene, *cis*-decalin, dibutyl phthalate, and dioctyl phthalate at 15.37 and 76.86 MHz (5 pages). Ordering information is given on any current masthead page.

References and Notes

- (1) Kramers, H. A. *Physica* **1940**, *7*, 284.
- (2) Helfand, E. J. *J. Chem. Phys.* **1971**, *54*, 4651.
- (3) Zhu, W.; Gisser, D. J.; Ediger, M. D. *J. Polym. Sci., Polym. Phys. Ed.* **1994**, *32*, 2251.
- (4) Glowinkowski, S.; Gisser, D. J.; Ediger, M. D. *Macromolecules* **1990**, *23*, 3520.
- (5) Zhu, W.; Ediger, M. D. *Macromolecules* **1995**, *28*, 7549.
- (6) Tylanakis, E. I.; Dais, P.; Heatley, F. *J. Polym. Sci., Polym. Phys. Ed.* **1997**, *35*, 317.
- (7) Zhu, W.; Ediger, M. D. *J. Polym. Sci., Polym. Phys. Ed.*, in press.
- (8) Heatley, F. *Prog. Nucl. Magn. Reson. Spectrosc.* **1979**, *13*, 47 and references therein.
- (9) Viswanath, D. S.; Natarajan, G. *Data Book on the Viscosity of Liquids*; Hemisphere Publishing: New York, 1989.
- (10) *International Critical Tables*; Washburn, E. W., West, C. J., Dorsey, N. E., Ring, M. D., Eds.; McGraw-Hill: New York, 1930; Vol. VII, p 211.
- (11) Barlow, A. J.; Lamb, J.; Matheson, A. J. *Proc. R. Soc. London A* **1966**, *292*, 322.
- (12) Laupretre, F.; Noel, C.; Monnerie, L. *J. Polym. Sci., Polym. Phys. Ed.* **1977**, *15*, 2143.

- (13) In ref 7, we calculate the average ^{13}C T_1 for both kinds of backbone carbons from the fitting of deuterium T_1 values. These calculated ^{13}C T_1 data are found to be consistent with literature values for the methine carbon. Thus the assumption that the two kinds of C–D vectors behave similarly is further justified.
- (14) Often the correlation time is given the symbol τ_c . Here $\langle o \rangle$ is used to represent the time integral of the correlation function. This is to emphasize that the integral is a model-independent quantity.
- (15) Bovey, F. A. *Nuclear Magnetic Resonance Spectroscopy*, 2nd ed.; Academic Press: San Diego, CA, 1988.
- (16) Abragam, A. *The Principles of Nuclear Magnetism*, Clarendon Press: Oxford, 1961; Chapter VIII.
- (17) Loewenstein, A. *Advances in Nuclear Quadrupole Resonance*, John Wiley & Sons: London, New York, 1983; Vol. 5.
- (18) Lucken, E. A. C. *Nuclear Quadrupole Coupling Constants*, Academic Press: London, New York, 1969.
- (19) Dais, P.; Spyros, A. *Prog. Nucl. Magn. Reson. Spectrosc.* **1995**, 27, 555.
- (20) Heatley, F. *Annu. Rep. NMR Spectrosc.* **1986**, 17, 179.
- (21) Gronski, W.; Schaefer, T.; Peter, R. *Polym. Bull.* **1979**, 1, 319.
- (22) Mashimo, S. *Macromolecules* **1976**, 9, 91.
- (23) Lang, M. C.; Laupretre, F.; Noel, C.; Monnerie, L. *J. Chem. Soc., Faraday Trans.* **1979**, 275, 349.
- (24) Spyros, A.; Dais, P.; Heatley, F. *Macromolecules* **1994**, 27, 6207.
- (25) Grote, R. F.; Hynes, J. T. *J. Chem. Phys.* **1980**, 73, 2715.
- (26) Bagchi, B.; Oxtoby, D. *J. Chem. Phys.* **1983**, 78, 2735.
- (27) Biswas, R.; Bagchi, B. *J. Chem. Phys.* **1996**, 105, 7543.
- (28) Moe, N. E.; Ediger, M. D. *Macromolecules* **1996**, 29, 5484.
- (29) Grandjean, J.; Sillescu, H.; Willenberg, B. *Makromol. Chem.* **1977**, 178, 1445.
- (30) Waldow, D. A.; Ediger, M. D.; Yamaguchi, Y.; Matsushita, Y.; Noda, I. *Macromolecules* **1991**, 24, 3147.
- (31) Adolf, D. B.; Ediger, M. D.; Kitano, T.; Ito, K. *Macromolecules* **1992**, 25, 867.

MA961426U